

The global electroweak Standard Model fit after the Higgs discovery

M. Baak^a, R. Kogler^b (for the Gfitter group)

^a*CERN, Geneva, Switzerland*

^b*Institut für Experimentalphysik, Universität Hamburg, Germany*

We present an update of the global Standard Model (SM) fit to electroweak precision data under the assumption that the new particle discovered at the LHC is the SM Higgs boson. In this scenario all parameters entering the calculations of electroweak precision observables are known, allowing, for the first time, to over-constrain the SM at the electroweak scale and assert its validity. Within the SM the W boson mass and the effective weak mixing angle can be accurately predicted from the global fit. The results are compatible with, and exceed in precision, the direct measurements. An updated determination of the S , T and U parameters, which parametrize the oblique vacuum corrections, is given. The obtained values show good consistency with the SM expectation and no direct signs of new physics are seen. We conclude with an outlook to the global electroweak fit for a future e^+e^- collider.

1 Introduction

The electroweak fit of the Standard Model (SM) has a long tradition in particle physics. It relies on the predictability of the SM, where all electroweak observables can be expressed as functions of five parameters. A tremendous amount of pioneering work from the theoretical community in the calculation of radiative corrections, as well as from the experimental community in the measurement of electroweak precision observables, led to a correct prediction [1] of the top-quark mass m_t before its actual discovery in 1995 [2, 3]^a. This success has given confidence in the calculations of radiative corrections, including loop-contributions from the Higgs boson.

The discovery of the top quark left the Higgs boson mass M_H as the last free parameter of the SM without experimental constraints. The focus of the electroweak fits shifted to precisely predicting M_H from electroweak precision observables (EWPO). However, while the loop corrections to the W - and Z -propagators involving the top quark lead to an approximate quadratic dependence, M_H enters only logarithmically in the calculation of electroweak observables, leading to weaker constraints on M_H than on m_t . Nevertheless, improvements in theoretical and experimental precision, especially on m_b , M_W and the hadronic contribution to the running of the electromagnetic coupling for the five light quarks $\Delta\alpha_{\text{had}}^{(5)}(s)$, led to a rather precise SM prediction of $M_H = 96_{-24}^{+31}$ GeV [5].

This was the status of the electroweak fit at the discovery of the new Higgs-like boson reported by the ATLAS and CMS collaborations [6, 7]. The predicted value is in very good agreement with its measured mass of ~ 126 GeV. Most recent measurements and analyses of the properties of this newly discovered boson, as presented at this conference, show good consistency with the assumption that the new particle is indeed the SM Higgs boson [8].

^a The observed top quark mass was $176 \pm 8(\text{stat}) \pm 10(\text{sys.})$ GeV and $199_{-21}^{+19}(\text{stat.}) \pm 22(\text{sys.})$ GeV as measured by the CDF and D0 collaborations. This is in very good agreement with the SM prediction of $m_t = 178_{-22}^{+18}$ GeV [4], as obtained from electroweak precision data.

Supposing that the new particle is the SM Higgs boson, all parameters entering electroweak precision observables are known, allowing a full assessment of the consistency of the SM at the electroweak scale [9]. We interpret the new particle as the SM Higgs boson and present an update of the SM electroweak fit using the Gfitter framework [10]. The Gfitter results shown here have been recently published elsewhere [11].

A detailed study of the implications of the value of M_H as input to the electroweak fit shows an improvement in precision on the predictions of M_W and the effective weak mixing angle $\sin^2\theta_{\text{eff}}^\ell$. We also report updated constraints on the oblique parameters S, T, U , which parametrize possible contributions to oblique vacuum corrections from physics beyond the SM (BSM) and hence allow to constrain new models through EWPO. We also use the projected experimental uncertainties from a future e^+e^- facility to derive the expected precision of SM predictions for electroweak observables.

2 The global electroweak fit with Gfitter

A detailed description of the calculations and experimental input used in the electroweak fit is given elsewhere [11] and only the most important features are given here. The mass of the W boson and the effective weak mixing angle are calculated at two-loop order, including leading terms beyond the two loop calculation [12–14]. We use the full $\mathcal{O}(\alpha_s^4)$ calculation [15, 16] of the QCD Adler function, which stabilizes the perturbative QCD expansion in the calculation of the Z -boson width. An improved prediction of R_b^0 , the hadronic partial decay width of $Z \rightarrow b\bar{b}$, is used, which includes the complete calculation of fermionic two-loop corrections [17]. The calculation of the vector and axial-vector couplings, g_A^f and g_V^f , used in the calculation of the partial and total widths of the Z and W bosons, relies on accurate parametrizations [18–21]. Theoretical uncertainties are implemented using the R fit scheme, which corresponds to a linear addition of theoretical and experimental uncertainties. The two uncertainties considered are due to missing higher orders in the calculations of M_W and $\sin^2\theta_{\text{eff}}^\ell$ and have been estimated to be $\delta_{\text{th}}M_W = 4 \text{ MeV}$ [12] and $\delta_{\text{th}}\sin^2\theta_{\text{eff}}^\ell = 4.7 \cdot 10^{-5}$ [13].

The experimental input used in the fit include the electroweak precision data measured at the Z -pole together with their correlations [22]. For the mass and width of the W boson the latest world average is used, $M_W = 80.385 \pm 0.015 \text{ GeV}$ and $\Gamma_W = 2.085 \pm 0.042 \text{ GeV}$, obtained from measurements by the LEP and Tevatron experiments [23]. While the leptonic contribution to the running of the electromagnetic coupling strength can be calculated with very high precision, the value of the hadronic contribution is obtained from a fit to experimental data supplemented by perturbative calculations, $\Delta\alpha_{\text{had}}^{(5)}(M_Z^2) = (2757 \pm 10) \cdot 10^{-5}$ [24].

For the mass of the top quark we use the average from the direct measurements by the Tevatron experiments $m_t = 173.18 \pm 0.94 \text{ GeV}$ [25]. Biases in the measurement of m_t due to a mis-modeling of non-perturbative color-reconnection effects in the fragmentation process, initial and final state radiation and kinematics of the b -quark, have been studied by the CMS collaboration [26]. With the current precision no significant deviation is observed between the measured values and the predictions using different models. An additional ambiguity in the interpretation of m_t originates from the top's finite decay width, with additional uncertainty which is difficult to estimate quantitatively. The effect of an additional theoretical uncertainty of 0.5 GeV on m_t has been studied, and the fit shows only a slight deterioration in precision. This uncertainty is not included in the standard fit setup.

A naïve combination of the measured values of M_H from the ATLAS and CMS experiments as reported in [6, 7], gives $M_H = 125.7 \pm 0.4 \text{ GeV}$, where the systematic uncertainties are treated as fully uncorrelated. Treating them as fully correlated only changes the uncertainty to 0.5 GeV, with a negligible effect on the fit result due to the weak dependence on, M_H .

3 The SM fit

The SM electroweak fit is performed in three scenarios [11]. In the first scenario all input parameters are used, allowing to test the validity of the SM. The results are compared to the second scenario, where the fit is performed without the inclusion of M_H to assess the effect of knowing M_H in the electroweak fit. In the third scenario individual observables are removed one by one from the fit which allows for an indirect determination of these with an accurate uncertainty calculation.

The SM fit including all input data converges with a minimum value of the test statistics of $\chi^2_{\min} = 21.8$, obtained for 14 degrees of freedom. Calculating the naïve p -value gives $\text{Prob}(21.8, 14) = 0.08$. The smallness of the p -value with respect to previous results [5] is not due to the inclusion of M_H , but rather due to the new calculation of R_b^0 which has a very small dependence on M_H , as described below.

Performing the fit without M_H as input parameter, the fit converges at a minimum of $\chi^2_{\min} = 20.3$ for 13 degrees of freedom, corresponding to a p -value of 0.09. In this case the fit converges for a value of $M_H = 94^{+25}_{-22}$ GeV, in good agreement with the direct measurement.

The result of the fit is shown in Fig. 1 in terms of the pull value, which is defined as deviation between the SM prediction and the measured parameter in units of the measurement uncertainty. The fit results are shown for both scenarios, including the M_H measurement (colored bars) and without M_H (grey bars), where in general the result of the fit does not change significantly between the two scenarios. Very small pull values, as for example observed for the light quark masses but also for M_H , indicate that the input accuracy exceeds the fit requirements. No single pull value exceeds 3σ , showing an overall satisfying consistency of the SM.

The largest deviations between the SM prediction and the measurements are observed in the b -sector. Both observables directly sensitive to $Z \rightarrow b\bar{b}$, the forward-backward asymmetry $A_{\text{FB}}^{0,b}$ and the partial width R_b^0 , show large deviations of 2.5σ and -2.4σ , respectively. While the effect in $A_{\text{FB}}^{0,b}$ has been known for a long time, the large deviation in R_b^0 is new, owing to the improved two-loop calculation which exhibits an unexpected large negative correction [17]. Using the one-loop result for R_b^0 only, the pull value is -0.8σ . Both parameters show only very little dependence on the inclusion of M_H , with deviations of 2.7σ and -2.3σ in the fit scenario without including M_H .^b

In order to assess the validity of the fit we use Monte Carlo simulation to generate pseudo experiments. For each simulation we generate SM parameters according to Gaussian distributed values around their expected values with standard deviations equal to the full experimental uncertainty. The obtained χ^2_{\min} distribution for all toy datasets is shown in Fig. 2(a). Good agreement between the MC simulation and the idealized distribution for 14 degrees of freedom

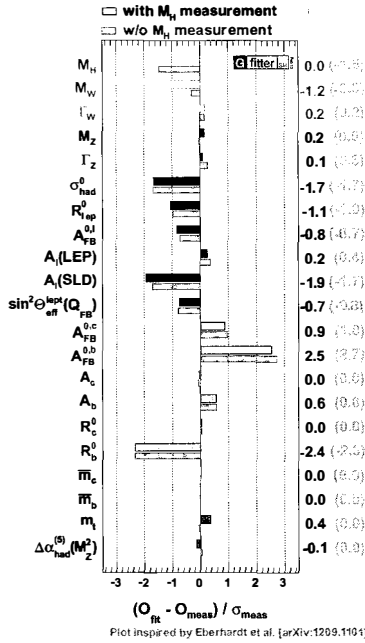


Figure 1: Differences between the SM prediction and the measured parameter, in units of the uncertainty for the fit including M_H (color) and without M_H (grey).

^b It is intriguing to observe that an increase of the right-handed coupling of the $Z \rightarrow b\bar{b}$ vertex of 25%, while leaving the left-handed coupling unchanged, can resolve both deviations.

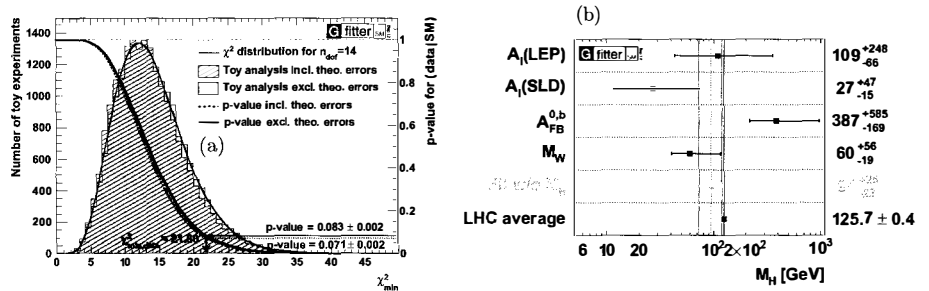


Figure 2: Distribution of the χ^2_{\min} value obtained from pseudo Monte Carlo simulations (a). Shown are distributions obtained by including (hatched) and excluding (green) the theory uncertainties δ_{th} , compared with the idealized χ^2 distribution assuming Gaussian distributed errors with 14 degrees of freedom. The arrows indicate the χ^2_{\min} value obtained from the fit to data. The result from a determination of M_H using only the given observable is shown in (b).

is found. The result from the fit to data is indicated as red arrow and the obtained p -value is consistent between the MC simulation and the idealized χ^2 distribution. The influence of the theoretical uncertainties on the p -value of the full SM fit amounts to about 0.01.

Except for the value of M_H itself, the largest change in the result due to the inclusion of M_H is the prediction of M_W . For this observable the pull value changes from -0.3 to -1.2 , due to the small value of M_H preferred by the M_W measurement. This effect is shown in Fig. 2(b), where indirect determinations of M_H are displayed, obtained by removing all sensitive observables from the fit except the given one. For comparison, also the indirect fit result using all input parameters except for M_H (grey band) and the direct measurement (green line) are shown. The values obtained from the fit including the measurements of the leptonic asymmetries A_ℓ , as measured by the LEP and SLD collaborations, and M_W show good agreement. The value of M_H obtained from the hadronic forward-backward asymmetry $A_{\text{FB}}^{0,b}$ shows a tendency towards large values of M_H , with a discrepancy of 2.5σ .

4 Predictions for key observables

The inclusion of M_H in the fit results in a large improvement in precision for the indirect determination of several SM parameters. Without the inclusion of M_H , the indirect determination of the top mass gives $m_t = 171.5^{+8.9}_{-5.3}$ GeV. Including the knowledge about M_H , the fit value obtained is

$$m_t = 175.8^{+2.7}_{-2.4} \text{ GeV}, \quad (1)$$

where the uncertainty is reduced by a factor of 2–3. The value of m_t agrees well with the direct determination [25] and the cross-section based determination under the assumption that there is no new physics contributing to the cross section measurement [27].

The $\Delta\chi^2$ profiles versus M_W and $\sin^2\theta_{\text{eff}}^\ell$ without using the corresponding measurements are shown in Fig. 3. For the indirect determination of $\sin^2\theta_{\text{eff}}^\ell$ all observables directly sensitive to $\sin^2\theta_{\text{eff}}^\ell$, like asymmetry parameters and the full and partial decay widths, are excluded from the fit. Solid blue lines show the result of the fit including M_H , where the effect of the theory uncertainty is shown as blue band. The same fit, without information on M_H is shown in grey. An improvement in precision of more than a factor of two can be observed for the indirect determination of M_W and $\sin^2\theta_{\text{eff}}^\ell$. Also shown are the direct measurements of the aforementioned W mass and the LEP/SLD average of the effective weak mixing angle $\sin^2\theta_{\text{eff}}^\ell = 0.23153 \pm 0.00016$ [22], which show good agreement with the obtained values.

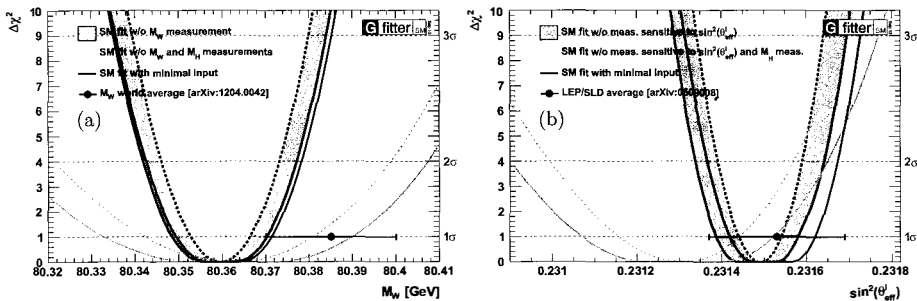


Figure 3: $\Delta\chi^2$ profiles for the indirect determination of M_W (a) and $\sin^2\theta_{\text{eff}}^\ell$ (b). The result from a fit including M_H as input parameter is shown in blue and the fit without M_H is shown in grey. The dotted lines indicate the fit result by setting the theoretical uncertainties δ_{th} to zero and the band corresponds to the full result. Also shown are the direct measurements and the SM prediction using a minimal set of parameters (black solid lines).

The fit value obtained for M_W is

$$\begin{aligned}
 M_W &= (80.3593 \pm 0.0056_{m_t} \pm 0.0026_{M_Z} \pm 0.0018_{\Delta\alpha_{\text{had}}} \\
 &\quad \pm 0.0017_{\alpha_S} \pm 0.0002_{M_H} \pm 0.0040_{\text{theo}}) \text{ GeV}, \\
 &= (80.359 \pm 0.011_{\text{tot}}) \text{ GeV},
 \end{aligned} \tag{2}$$

which exceeds the experimental world average in precision. The different uncertainty contributions originate from the uncertainties in the input values of the fit. The dominant uncertainty is due to the top quark mass, followed by the theory uncertainty of 4 MeV. Due to the weak, logarithmic dependence on M_H the contribution from the uncertainty on the Higgs mass is very small compared to the other sources of uncertainty. The deviation between the value of M_W obtained from the fit and the direct measurement is not significant with the current precision (1.2σ). However, improvements in the determination of m_t as well as reduced theoretical uncertainties from higher-order calculations and a more precise direct determination of M_W – as expected from the analyses of the full dataset recorded by the Tevatron experiments – will reduce the uncertainties significantly.

The indirect determination of $\sin^2\theta_{\text{eff}}^\ell$ gives

$$\begin{aligned}
 \sin^2\theta_{\text{eff}}^\ell &= 0.231496 \pm 0.000030_{m_t} \pm 0.000015_{M_Z} \pm 0.000035_{\Delta\alpha_{\text{had}}} \\
 &\quad \pm 0.000010_{\alpha_S} \pm 0.000002_{M_H} \pm 0.000047_{\text{theo}}, \\
 &= 0.23150 \pm 0.00010_{\text{tot}},
 \end{aligned} \tag{3}$$

which is compatible and more precise than the average of the LEP/SLD measurements. The total uncertainty is dominated by that from the measurements of $\Delta\alpha_{\text{had}}$ and m_t . The contribution from the uncertainty in M_H is again very small.

The measurement of M_H allows for a first time to predict SM observables with a minimal set of parameters. A fit using only this minimal set of input measurements (here chosen to be M_H , $\alpha_S(M_Z^2)$, the fermion masses and M_Z , G_F and $\Delta\alpha_{\text{had}}^{(5)}(M_Z^2)$ for the electroweak sector) is shown by the solid black lines in Fig. 3. The agreement in central value and precision of these results with those from Eq. (2) and (3) illustrates the marginal additional information provided by the other observables once M_H is known.

An important consistency test of the SM is the simultaneous, indirect determination of m_t and M_W . This is particularly interesting since contributions from new physics may lead to

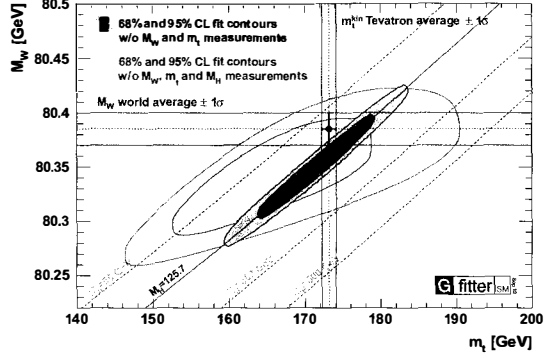


Figure 4: 68% and 95% confidence level (CL) contours in the m_t - M_W plane for the fit including M_H (blue) and excluding M_H (grey). In both cases the direct measurements of M_W and m_t were excluded from the fit. The values of the direct measurements are shown as green bands with their one standard deviations. The dashed diagonal lines show the SM prediction for M_W as function of m_t for different assumptions of M_H .

discrepancies between the measured values and the predictions in the m_t - M_W plane. A scan of the $\Delta\chi^2$ profile is shown in Fig. 4 for the scenario including M_H in the fit (blue) and without M_H (grey). The knowledge of M_H improves the precision of the indirect determination of M_W and m_t significantly. Very good agreement between the indirect determinations of M_W and m_t and the direct measurements is observed, showing impressively the consistency of the SM and leaving little room for signs of new physics.

5 Oblique Parameters

If the scale of new physics (NP) is much higher than the mass of the W and Z bosons, beyond the SM physics appears dominantly through vacuum polarization corrections, also known as oblique corrections, in the calculation of EWPO. Their effects on the electroweak precision observables can be parametrized by three gauge self-energy parameters (S , T , U) introduced by Peskin and Takeuchi [28, 29]. The parameter S describes new physics contributions to neutral current processes at different energy scales. T is sensitive to isospin violation and U ($S+U$) is sensitive to new physics (NP) contributions to charged currents. U is only sensitive to the W mass and width, and is usually very small in NP models (often: $U=0$).

Constraints on the S , T , U parameters are derived from the global fit to the electroweak precision data, namely from the difference between the oblique vacuum corrections determined from the experimental data and the corrections expected in a reference SM (defined by fixing m_t and M_H). The reference SM for the S , T , U calculation is now updated to $M_{H,\text{ref}} = 126$ GeV and $m_{t,\text{ref}} = 173$ GeV. With this one finds for S , T , U :

$$S = 0.03 \pm 0.10, \quad T = 0.05 \pm 0.12, \quad U = 0.03 \pm 0.10, \quad (4)$$

with correlation coefficients of +0.89 between S and T , and -0.54 (-0.83) between S and U (T and U). Fixing $U=0$ one obtains $S|_{U=0} = 0.05 \pm 0.09$ and $T|_{U=0} = 0.08 \pm 0.07$, with a correlation coefficient of +0.91.

Fig. 5 shows the 68%, 95% and 99% CL allowed regions in the (S, T) plane for freely varying U (a) and the constraints found when fixing $U=0$ (b). For illustration purposes, also the SM prediction is shown. The M_H measurement reduces the allowed SM area from the grey sickle, defined by letting M_H float within the range of [100, 1000] GeV, to the narrow black strip. The

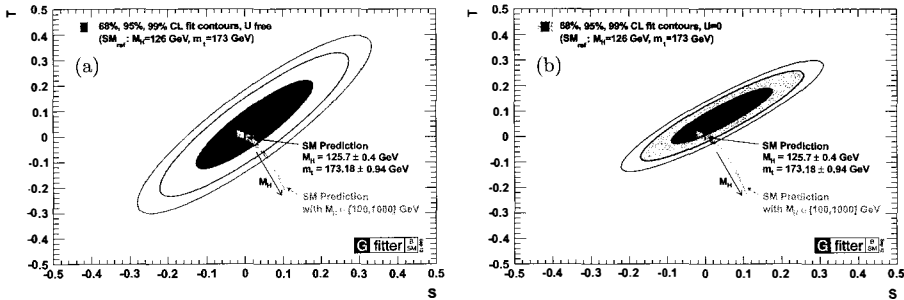


Figure 5: Experimental constraints on the S and T parameters with respect to the SM reference ($M_{H,\text{ref}} = 126$ GeV and $m_{t,\text{ref}} = 173$ GeV). Shown are the 68%, 95% and 99% CL allowed regions, where the third parameter U is left unconstrained (a) or fixed to 0 (b). The prediction in the SM is given by the black (grey) area when including (excluding) the M_H measurements.

experimental constraints on S , T , U can be compared now to specific NP model predictions. Since the oblique parameters are found to be small and consistent with zero, possible NP models may only affect the electroweak observables weakly.

6 Prospects of the SM fit for a future e^+e^- collider

The SM leaves many questions open which can only be addressed by BSM physics, which is expected to play a role at the electroweak scale of $\mathcal{O}(1)$ TeV. So far no direct signs of new physics have been observed at the LHC and also the SM shows good self-consistency at the loop-level up to very high precision. A future e^+e^- facility would help tremendously to precisely measure the production mechanisms and branching ratios of the Higgs boson. Furthermore, it would allow for precise measurements of the EWPO, such as m_t , $\sin^2\theta_{\text{eff}}^\ell$, R_ℓ^0 and M_W , to further assert the validity of the SM through the electroweak fit.

In the following we study the impact of expected EWPO measurements on the SM electroweak fit assuming the design parameters and predicted precisions obtained for the International Linear Collider (ILC) with the GigaZ option [30–32]. This study aims at a comparison of the accuracies of the measured and predicted electroweak observables. Two scenarios are considered. In the first scenario the central values of the input observables are chosen to agree with the SM prediction for a Higgs mass of 125.8 GeV according to the present measurement. In the second scenario it is assumed that the central value of the SM prediction for M_H does not change and all SM parameters are chosen to agree with $M_H = 94$ GeV.

Total experimental uncertainties of 6 MeV for M_W , $13 \cdot 10^{-5}$ for $\sin^2\theta_{\text{eff}}^\ell$, $4 \cdot 10^{-3}$ for R_ℓ^0 , and 100 MeV for m_t (interpreted as pole mass) are assumed [31]. The exact achieved precision on the Higgs mass is irrelevant for this study. For the hadronic contribution to the running of the QED fine structure constant at the Z pole, $\Delta\alpha_{\text{had}}^{(5)}(M_Z^2)$, an uncertainty of $4.7 \cdot 10^{-5}$ is assumed,^c compared to the currently used uncertainty of $10 \cdot 10^{-5}$ [24]. The other input observables to the electroweak fit are taken to be unchanged from the current settings.

The most important theoretical uncertainties in the fit are those affecting the M_W and $\sin^2\theta_{\text{eff}}^\ell$ predictions arising from unknown higher-order corrections. We assume in the following that theoretical developments have led to improved uncertainties of only half the present values,

^c The uncertainty on $\Delta\alpha_{\text{had}}^{(5)}(M_Z^2)$ will benefit below the charm threshold from the completion of BABAR analyses and the ongoing program at VEPP-2000. At higher energies improvements are expected from charmonium resonance data from BES-3, and a better knowledge of α_s from the R_ℓ^0 measurement and reliable lattice QCD predictions [33].

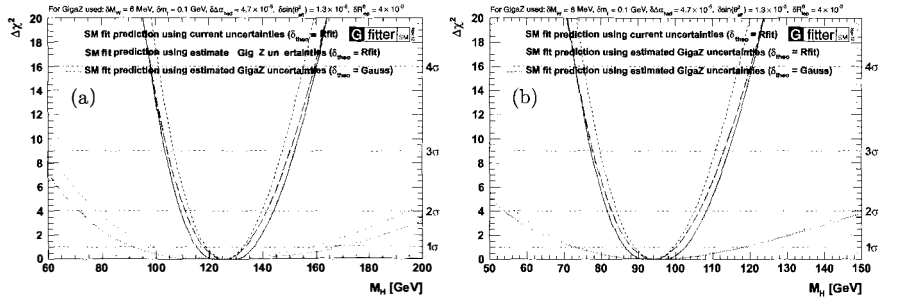


Figure 6: ILC projection of the $\Delta\chi^2$ profiles as a function of the Higgs mass for electroweak fits compatible with an SM Higgs boson of mass 125.8 GeV (a) and 94 GeV (b). The measured Higgs boson mass is not used as input in the fit. The grey bands show the results obtained using present uncertainties [11], and the yellow bands indicate the results for the hypothetical future scenario (a) and corresponding input data shifted to accommodate a 94 GeV Higgs boson but unchanged uncertainties (b). The thickness of the bands indicates the effect from the theoretical uncertainties treated according to the *Rfit* prescription. The long-dashed line in each plot shows the curves when treating the adding the theoretical uncertainties in according to Gaussian distributed values.

$$\delta_{\text{th}} M_W = 2 \text{ MeV} \text{ and } \delta_{\text{th}} \sin^2 \theta_{\text{eff}}^{\ell} = 1.5 \cdot 10^{-5}.$$

The indirect prediction of the Higgs mass at 126 GeV achieves an uncertainty of $^{+12}_{-10}$ GeV. Keeping the present theoretical uncertainties in the prediction of M_W and $\sin^2 \theta_{\text{eff}}^{\ell}$ would worsen the accuracy of the M_H prediction to $^{+20}_{-17}$ GeV, whereas neglecting theoretical uncertainties altogether would improve it to ± 7 GeV. This emphasizes the importance of theoretical updates.

For M_W the prediction with an estimated uncertainty of 5 MeV is similarly accurate as the assumed measurement, while the prediction of $\sin^2 \theta_{\text{eff}}^{\ell}$ with an uncertainty of $4 \cdot 10^{-5}$ is three times less accurate than the expected experimental precision. The fit would therefore particularly benefit from additional experimental improvement in M_W . The accuracy of the indirect determination of the top mass is 1.2 GeV, which is similar to that of the present experimental determination. The fit would therefore benefit significantly from a reduction of the uncertainty on m_t to a value of about 100 MeV. The measurement of the strong coupling constant with an experimental uncertainty of 0.4% and a theoretical uncertainty of only 0.1%, which has been achieved already today owing to the full $\mathcal{O}(\alpha_s^4)$ calculation of the QCD Adler function [15, 16].

Profiles of $\Delta\chi^2$ as a function of the Higgs mass for present and future electroweak fits compatible with a SM Higgs boson of mass 125.8 GeV and 94 GeV are shown in Fig. 6(a) and (b), respectively. The measured Higgs boson mass is not used as input in these fits. If the experimental input data, currently predicting $M_H = 94^{+25}_{-22}$ GeV, were left unchanged with respect to the present values, but had uncertainties according to the ILC expectations, a deviation of the measured M_H exceeding 4σ could be established with the fit, see Fig. 6(b). Such a conclusion does not strongly depend on the treatment of the theoretical uncertainties (*Rfit* versus Gaussian, i.e. quadratic addition) as can be seen by comparison of the solid yellow and the long-dashed yellow $\Delta\chi^2$ profiles.

Additionally to establishing a precise statement about the compatibility of the directly measured value of M_H and the SM prediction, the high precision measurements of EWPO at the ILC would significantly improve the indirect determination of SM parameters which has a high sensitivity to additional contributions of new physics on the loop-level and complements direct searches for new physics. Prospects for the precision of the simultaneous indirect determination of m_t and M_W are shown in Fig. 7(a) together with the present and expected precision of the m_t and M_W measurements. The gain in precision of the indirect measurements is about a factor

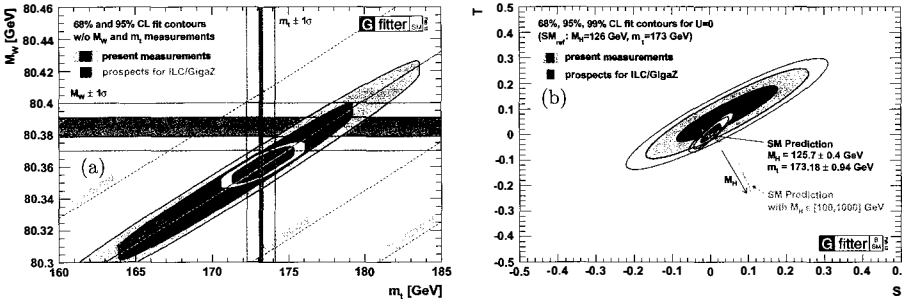


Figure 7: ILC projection of the contour lines of 68%, 95% CL allowed regions in the m_t – M_H plane. Shown are the current indirect determinations (blue) and the expected precision using prospects for ILC measurements of EWPO (orange). The present direct measurements together with the experimental uncertainties are shown as light green bands, the prospects for the uncertainties on m_t and M_H are shown as dark green bands. Contour lines of 68%, 95% and 99% CL allowed regions on the S and T parameters for $U = 0$ with respect to the SM reference ($M_{H,ref} = 126$ GeV and $m_{t,ref} = 173$ GeV) (b). The prediction in the SM is given by the black (grey) area when including (excluding) the M_H measurements.

of three with respect to the current determinations. Assuming that the central values of m_t and M_W do not change from their present values, a deviation between the SM prediction and the direct measurements would be prominently visible.

The precisely measured EWPO would also help to constrain new physics through oblique corrections. The expected constraints on the S and T parameters are shown in Fig. 7(b), where an improvement of more than a factor of 3 seems to be possible.

7 Conclusion

Assuming the newly discovered particle at ~ 126 GeV to be the Standard Model (SM) Higgs boson, all SM parameters entering electroweak precision observables are known. For the first time, the fit can over-constrain the SM at the electroweak scale and evaluate its validity. We reported here on the most recent results from the electroweak fit [11].

The measured value of the Higgs mass agrees at 1.3σ with the indirect prediction from the electroweak fit. The global fit to all the electroweak precision data and the measured Higgs mass results in a goodness-of-fit p -value of 7%. Only a fraction of the contribution to the “incompatibility” stems from the Higgs mass. The largest deviation between the best fit result and the data is introduced by $A_{FB}^{0,b}$ – a known tension – and by R_b^0 . A revisit of these two quantities would be very interesting, both theoretically and experimentally.

The knowledge of the Higgs mass dramatically improves the SM predictions of several key observables, in particular of the top mass, the W -mass, and $\sin^2\theta_{eff}^\ell$. The predicted uncertainties decrease by a factor of ~ 2.5 , from 6.2 to 2.5 GeV, 28 to 11 MeV, and $2.3 \cdot 10^{-5}$ to $1.0 \cdot 10^{-5}$ respectively. Theoretical uncertainties due to unknown higher-order electroweak and QCD corrections contribute approximately half of the uncertainties in the M_W and $\sin^2\theta_{eff}^\ell$ predictions.

The observed agreement of these quantities between the indirect determinations and measurements demonstrates the impressive consistency of the SM. The improved accuracy of the indirect determination of M_W sets a benchmark for new direct measurements.

Updated values for the oblique parameters S , T , U have been presented, using the measured value of the Higgs mass as a reference, and indicate that possible new physics models may affect the electroweak observables only weakly.

Finally, the perspectives of the electroweak fit considering a future e^+e^- collider running

also at energies at the Z-pole have been analyzed. Assuming a good control over systematic effects results in improved accuracy of the predictions for the top mass, the W -mass, $\sin^2\theta_{\text{eff}}^\ell$ and $\alpha_s(M_Z^2)$ with a factor of three or greater. We point out that, in order to fully exploit the experimental potential, theoretical developments are mandatory, in particular in the accuracy of M_W and $\sin^2\theta_{\text{eff}}^\ell$, requiring the calculation of higher order electroweak and QCD corrections.

References

- [1] The ALEPH, DELPHI, L3, OPAL Collaborations, the LEP Electroweak Working Group, (1995), CERN-PPE-95-172.
- [2] CDF Collaboration, F. Abe *et al.*, Phys. Rev. Lett. **74**, 2626 (1995), [hep-ex/9503002].
- [3] D0 Collaboration, S. Abachi *et al.*, Phys. Rev. Lett. **74**, 2632 (1995), [hep-ex/9503003].
- [4] C. Campagnari and M. Franklin, Rev. Mod. Phys. **69**, 137 (1997), [hep-ex/9608003].
- [5] M. Baak *et al.*, Eur. Phys. J. **C72**, 2003 (2012), [1107.0975].
- [6] ATLAS Collaboration, G. Aad *et al.*, Phys. Lett. B (2012), [1207.7214].
- [7] CMS Collaboration, S. Chatrchyan *et al.*, Phys. Lett. B (2012), [1207.7235].
- [8] B. Dumont, these proceedings (2013), [1305.4635].
- [9] O. Eberhardt *et al.*, Phys. Rev. Lett. **109**, 241802 (2012), [1209.1101].
- [10] H. Flacher *et al.*, Eur. Phys. J. **C60**, 543 (2009), [0811.0009], Err.-ibid. C71 (2011) 1718.
- [11] M. Baak *et al.*, Eur. Phys. J. **C72**, 2205 (2012), [1209.2716], regular updates at <http://cern.ch/gfitter>.
- [12] M. Awramik, M. Czakon, A. Freitas and G. Weiglein, Phys. Rev. **D69**, 053006 (2004), [hep-ph/0311148].
- [13] M. Awramik, M. Czakon and A. Freitas, JHEP **0611**, 048 (2006), [hep-ph/0608099].
- [14] M. Awramik, M. Czakon, A. Freitas and G. Weiglein, Phys. Rev. Lett. **93**, 201805 (2004), [hep-ph/0407317].
- [15] P. Baikov, K. Chetyrkin and J. H. Kuhn, Phys. Rev. Lett. **101**, 012002 (2008), [0801.1821].
- [16] P. Baikov, K. Chetyrkin, J. Kuhn and J. Rittinger, Phys. Rev. Lett. **108**, 222003 (2012), [1201.5804].
- [17] A. Freitas and Y.-C. Huang, JHEP **1208**, 050 (2012), [1205.0299].
- [18] K. Hagiwara, S. Matsumoto, D. Haidt and C. Kim, Z. Phys. **C64**, 559 (1994), [hep-ph/9409380], Order of authors changed in journal.
- [19] K. Hagiwara, Ann. Rev. Nucl. Part. Sci. **48**, 463 (1998).
- [20] G.-C. Cho and K. Hagiwara, Nucl. Phys. **B574**, 623 (2000), [hep-ph/9912260].
- [21] G.-C. Cho, K. Hagiwara, Y. Matsumoto and D. Nomura, JHEP **1111**, 068 (2011), [1104.1769].
- [22] The ALEPH, DELPHI, L3, OPAL, SLD Collaborations, the LEP Electroweak Working Group, the SLD Electroweak and Heavy Flavour Working Groups, Phys. Rept. **427**, 257 (2006), [hep-ex/0509008].
- [23] CDF Collaboration, D0 Collaboration, Tevatron Electroweak Working Group, [1204.0042].
- [24] M. Davier, A. Hoecker, B. Malaescu and Z. Zhang, Eur. Phys. J. **C71**, 1515 (2011), [1010.4180].
- [25] CDF Collaboration, D0 Collaboration, T. Aaltonen *et al.*, [1207.1069].
- [26] CMS Collaboration, S. Chatrchyan *et al.*, CMS-PAS-TOP-12-029 (2012).
- [27] S. Alekhin, A. Djouadi and S. Moch, Phys. Lett. **B716**, 214 (2012), [1207.0980].
- [28] M. E. Peskin and T. Takeuchi, Phys. Rev. Lett. **65**, 964 (1990).
- [29] M. E. Peskin and T. Takeuchi, Phys. Rev. **D46**, 381 (1992).
- [30] ECFA/DESY LC Physics Working Group, J. Aguilar-Saavedra *et al.*, hep-ph/0106315.
- [31] ILC Collaboration, G. Aarons *et al.*, 0709.1893.
- [32] ILD Concept Group - Linear Collider Collaboration, T. Abe *et al.*, 1006.3396.
- [33] M. Davier, *private communication*, Nov 2012.